



Transcriptomics Reveals How Minocycline-Colistin Synergy Overcomes Antibiotic Resistance in Multidrug-Resistant *Klebsiella pneumoniae*

 Thea Brennan-Krohn,^{a,c}  Alexandra Grote,^b  Shade Rodriguez,^a  James E. Kirby,^{a,c}  Ashlee M. Earl^b

^aDepartment of Pathology, Beth Israel Deaconess Medical Center, Boston, Massachusetts, USA

^bBroad Institute of MIT and Harvard, Cambridge, Massachusetts, USA

^cHarvard Medical School, Boston, Massachusetts, USA

Thea Brennan-Krohn and Alexandra Grote contributed equally to the manuscript and share first authorship. Author order was chosen based on initial conceptualization of the project by Thea Brennan-Krohn. James E. Kirby and Ashlee M. Earl share last authorship on this work.

ABSTRACT Multidrug-resistant Gram-negative bacteria are a rapidly growing public health threat, and the development of novel antimicrobials has failed to keep pace with their emergence. Synergistic combinations of individually ineffective drugs present a potential solution, yet little is understood about the mechanisms of most such combinations. Here, we show that the combination of colistin (polymyxin E) and minocycline has a high rate of synergy against colistin-resistant and minocycline-intermediate or -resistant strains of *Klebsiella pneumoniae*. Furthermore, using transcriptome sequencing (RNA-Seq), we characterized the transcriptional profiles of these strains when treated with the drugs individually and in combination. We found a striking similarity between the transcriptional profiles of bacteria treated with the combination of colistin and minocycline at individually subinhibitory concentrations and those of the same isolates treated with minocycline alone. We observed a similar pattern with the combination of polymyxin B nonapeptide (a polymyxin B analogue that lacks intrinsic antimicrobial activity) and minocycline. We also found that genes involved in polymyxin resistance and peptidoglycan biosynthesis showed significant differential gene expression in the different treatment conditions, suggesting possible mechanisms for the antibacterial activity observed in the combination. These findings suggest that the synergistic activity of this combination against bacteria resistant to each drug alone involves sublethal outer membrane disruption by colistin, which permits increased intracellular accumulation of minocycline.

KEYWORDS RNA-Seq, antibiotic resistance, antimicrobial activity, antimicrobial agents, antimicrobial combinations, antimicrobial synergy, transcriptomics

Colistin (also known as polymyxin E), a polypeptide antibiotic that was introduced in 1949, fell out of favor by the 1980s as the result of an unfavorable side effect profile notable for nephrotoxicity and neurotoxicity (1). Rising rates of multidrug resistance among Gram-negative bacterial pathogens, including carbapenem-resistant *Enterobacteriales* such as *Klebsiella pneumoniae*, subsequently led to a resurgence in the use of colistin due to its broad Gram-negative spectrum of activity. Inevitably, resistance to colistin emerged in the setting of increased use, leading to the appearance of pan-drug-resistant isolates (2, 3). Furthermore, colistin's clinical efficacy is hampered, even in treatment of susceptible isolates, by a low therapeutic index (4). Therefore, there is an urgent need to identify means of restoring the activity of colistin (and the closely related drug polymyxin B) against resistant bacteria and/or reducing the toxicity of the drug while retaining antimicrobial activity.

Structurally, colistin consists of two moieties—a cyclic polypeptide “head” and a

Copyright © 2022 American Society for Microbiology. All Rights Reserved.

Address correspondence to Thea Brennan-Krohn, tkrohn@bidmc.harvard.edu.

The authors declare no conflict of interest.

Received 5 October 2021

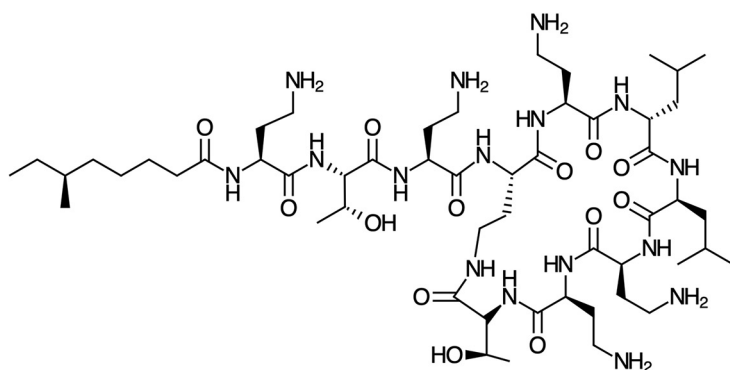
Returned for modification 10 November 2021

Accepted 11 January 2022

Accepted manuscript posted online 18 January 2022

Published 15 March 2022

Colistin (polymyxin E)



Polymyxin B

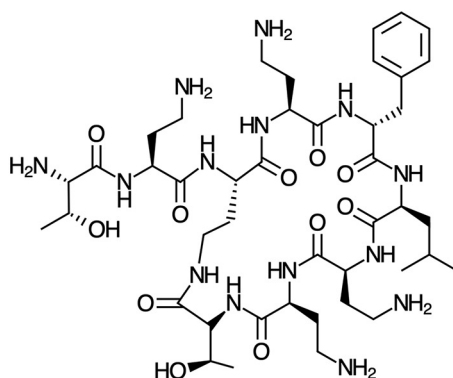


FIG 1 Chemical structure of colistin (polymyxin E) (top) and polymyxin B nonapeptide (PMBN) (bottom). Note the absence of the fatty acid tail in PMBN.

lipophilic fatty acid tail (Fig. 1). The drug's antibacterial activity results from a sequence of events that begins with binding of the polypeptide head to lipopolysaccharide (LPS) on the outer membrane of a Gram-negative bacterial cell, leading to outer membrane permeabilization. Colistin exposure ultimately results in disruption of the cytoplasmic membrane, leading to lysis and cell death. The exact mechanisms of these steps remain incompletely understood, but the process is believed to involve self-promoted uptake of the drug, possibly through insertion of the fatty acid tail into the hydrophobic interior of the outer membrane, as well as direct activity at the cytoplasmic membrane itself (Fig. 2) (5, 6). Colistin resistance results from modifications to the lipid A component of LPS that increase the charge of LPS, thereby impeding the molecule's electrostatic interaction with colistin (7). We have previously noted, however, that colistin exhibits robust synergistic activity (defined as a greater-than-additive effect when two drugs are used in combination [8]) against colistin-resistant strains when combined with antibiotics to which the strains are also resistant, including antibiotics that have no intrinsic Gram-negative activity (9).

One of the most consistently synergistic combinations we identified was colistin combined with the tetracycline derivative minocycline (9). This combination is active against the pan-drug resistant Nevada *K. pneumoniae* isolate (10) and other isolates that are resistant to both colistin and minocycline, demonstrating synergistic activity at low concentrations of both drugs against these strains. Like other tetracycline antibiotics, minocycline inhibits protein synthesis by binding to the 16S rRNA component of the 30S ribosomal subunit and inhibiting delivery of aminoacyl-tRNAs to the A-site, thereby blocking the elongation step (11). Minocycline has relatively broad intrinsic Gram-negative activity, but resistance, primarily due to efflux pump activity, is common.

The sensitization of colistin-resistant bacteria to intracellularly active antibiotics

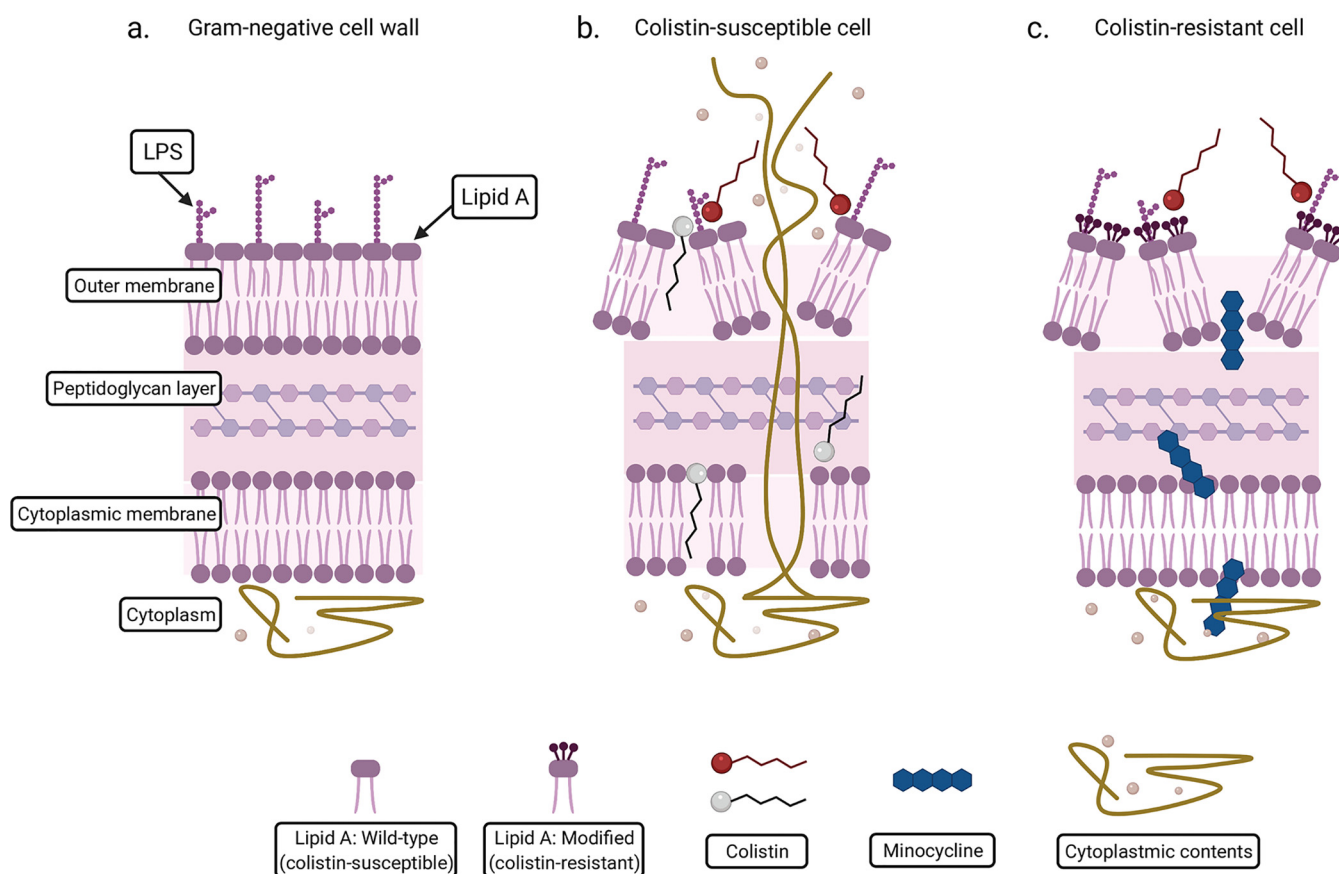


FIG 2 Diagram illustrating the mechanism of action of colistin. (a) A section of Gram-negative cell wall is shown (a). When a colistin-susceptible cell is exposed to colistin, permeabilization of the outer membrane, disruption of the cytoplasmic membrane, and cell lysis occur. Red colistin molecules illustrate colistin binding to the lipid A component of LPS. Gray colistin molecules indicate additional proposed activities of colistin, including insertion of the fatty acid tail into the membrane interior and activity at the cytoplasmic membrane (b). When a colistin-resistant cell is exposed to colistin, permeabilization of the outer membrane still occurs, allowing increased entry of minocycline. However, disruption of the cytoplasmic membrane and cell lysis do not occur (c).

such as minocycline appears analogous to the capacity of polymyxin B nonapeptide (PMBN) to sensitize Gram-negative bacteria to antibiotics that act in the intracellular compartment, despite lacking antibacterial activity on its own (12, 13). PMBN is a derivative of polymyxin B that retains the polypeptide head component of the antibiotic but lacks the fatty acid tail (Fig. 1); its activity in combinations is understood to be the result of a retained capacity for membrane disorganization (14). However, the precise mechanism by which loss of the fatty acid tail abrogates direct antibacterial activity while retaining permeabilizing capacity remains incompletely understood.

We hypothesized, by analogy, that synergistic activity in colistin-resistant strains is the result of subinhibitory outer membrane permeabilization, which allows increased intracellular accumulation of a drug administered in combination with colistin (Fig. 2) (9). In the case of minocycline, increased intracellular accumulation, in turn, would be sufficient to compensate for minocycline resistance mediated by efflux or other mechanisms. Alternatively, however, it is possible that colistin may have a separate, individually noninhibitory mechanism of action that is potentiated by the addition of a second antibiotic. It is critically important to elucidate the precise mechanisms of synergy in order to understand how synergistic combinations can be optimized and adopted for clinical use.

We therefore sought to address these alternative possibilities by harnessing the power of transcriptomic technologies. Transcriptome sequencing (RNA-Seq) is a tool that allows quantification of gene expression through sequencing of mRNA transcripts (15) and has been employed in a wide variety of organisms, including bacteria (16). Specifically, RNA-Seq can be used to profile and compare transcriptomic effects resulting from different

environmental exposures, and as such, it should offer a powerful way to compare and contrast the effects of antibiotics used alone or in synergistic combinations, thereby informing our understanding of synergistic activity. To date, there has been minimal use of RNA-Seq to study the activity of colistin or other polymyxin compounds on colistin-resistant bacteria (17, 18), and to our knowledge, there has been no previous investigation of the effect of colistin-containing combinations on gene expression in colistin-resistant *K. pneumoniae*. We used RNA-Seq transcriptomic analysis to study the effect of the combination of colistin and minocycline on *K. pneumoniae* isolates resistant to both drugs, as an understanding of the mechanism of action of this synergistic combination would provide valuable background and support for its potential clinical application.

RESULTS

The combination of minocycline and colistin shows high rates of synergy against colistin-resistant and minocycline-intermediate or -resistant strains using a checkerboard array assay. In order to characterize the activity of the combination of minocycline and colistin across a large number of *K. pneumoniae* strains with different genetic backgrounds and resistance profiles, we performed synergy testing on 219 deidentified clinical *K. pneumoniae* isolates (see Table S1 in the supplemental material), almost all of which have been sequenced (19), using an automated inkjet printer-assisted checkerboard array synergy assay validated in our laboratory (9, 20–22) and employed by the CDC for synergy testing of clinical isolates (23, 24). The combination was synergistic against 74/219 (34%) of strains overall and against 46/78 minocycline-intermediate or -resistant strains (59%) and 23/25 colistin-resistant strains (92%). Overall, the combination was significantly more likely to be synergistic against strains that were intermediate or resistant to one or both antibiotics than against those that were susceptible to both (590/91 [65%] versus 15/128 [12%]; $P < 0.001$). Similarly, among strains that were susceptible to colistin but intermediate or resistant to minocycline ($n = 66$), the modal minocycline MIC was $>32 \mu\text{g/mL}$ among strains against which the combination was synergistic but only $8 \mu\text{g/mL}$ among strains against which it was not synergistic (Table S1). Among the 12 strains that were intermediate or resistant to minocycline and resistant to colistin, the combination was synergistic against 10 (83%). For the other 2 strains, we observed both synergistic and antagonistic wells within the checkerboard array, so the combination was classified as having a mixed rather than synergistic effect. Mutations in genes related to colistin and tetracycline resistance in these 12 strains are detailed in Table 1 and Table S2. (The two strains in which the mixed phenotype occurred (FDA-CDC0040 and FDA-CDC0046; Table S_1) have similar underlying mechanisms for resistance to colistin (IS1 insertion sequence at nucleotide position 77 of the *mgrB* gene, the gene most commonly mutated in colistin-resistant *K. pneumoniae* [25]) and minocycline [presence of the *tet(A)* efflux pump]. Whole-genome comparisons revealed that these two strains are likely clones, having nearly identical chromosomes (differing only by a single nucleotide polymorphism, indels totaling 18 bp, and IS1 copy number) and the same complement of plasmids.

We also looked for a potentially clinically applicable “salvage” effect among the 10 strains that were intermediate or resistant to both drugs and against which the combination was synergistic. We considered a salvage effect to be present when the concentrations of the two drugs in the synergistic combination were not only reduced from their individually effective concentrations to a degree sufficient to classify them mathematically as synergistic, but were also clinically achievable; in 9/10 of the isolates, the concentrations of minocycline and colistin that were inhibitory in combination were each within the range that would be considered susceptible individually, suggesting potential clinical applicability of the combination for highly multidrug-resistant strains.

The combination of minocycline and colistin is synergistic in time-kill studies against MGH-149 and BIDMC-32. In order to explore the mechanism responsible for the synergistic killing of multidrug-resistant *K. pneumoniae* by minocycline and colistin, we examined the transcriptional responses of two unrelated colistin- and minocycline-resistant strains (MGH-149 and BIDMC-32; Tables 1 and 2). These strains were selected because they showed the strongest synergistic effect (i.e., lowest minimum fractional

TABLE 1 Resistance genes and mutations in strains used for transcriptomics^a

Strain ID	GenBank accession no.	CST MIC (ug/mL)	CST S//R	MIN MIC (ug/mL)	MIN S//R	FIC index	Min	Genes and mutations potentially conferring minocycline resistance				Mutations potentially conferring colistin resistance			
								Tet genes	ramR	acrR	oqxR	ompF (ompK35)	mgrB	phoP, phoQ, pmrA, pmrB, crrA, crrB	No predicted deleterious mutations identified in any isolates
MGH-149	GCA_002153115.1	> 16	R	32	R	0.063	1	0	tet(A)	T43M	None	None	None	Gene absent	
BIDMC-32	GCA_000567265.1	> 16	R	16	R	0.031	1	0	None	G96V	None	V130A	G41fs; V88*	nt G(-54)T	
BIDMC-5	GCA_000567445.1	0.5	S	8	I	0.5	1	0	None	G96V	None	V130A	G41fs; V88*	None	
MGH-64	GCA_000694515.1	0.25	S	1	S	1	0	0	None	None	None	None	None	None	

^aCST, colistin; MIN, minocycline; S, susceptible; I, intermediate; R, resistant. Interpretive criteria are defined according to EUCAST for colistin for susceptible; CLSI for others; see text for details. Min FIC index, lowest fractional inhibitory concentration index in the synergy grid; Syn, synergy; Ant, antagonism (1 = synergy/antagonism present in grid; 0 = synergy/antagonism not present in grid); nt, nucleotide.

TABLE 2 Strains used for transcriptomics^a

Strain ID	Sequence type	CST MIC (ug/mL)	CST interpretive category	CST low conc. (ug/mL)	CST high conc. (ug/mL)	MIN MIC (ug/mL)	MIN interpretive category	MIN low conc. (ug/mL)	MIN high conc. (ug/mL)	GenBank accession no.
MGH-149	ST-628	64	Resistant	1	64	32	Resistant	4	32	GCA_002153115.1
BIDMC-32	ST-258	32	Resistant	1	32	16	Resistant	1 (4 ^b)	16	GCA_000567265.1
BIDMC-5	ST-258	0.5	Susceptible	NA	NA	8	Intermediate	2 ^c	16	GCA_000567445.1
MGH-64	ST-35	0.25	Susceptible	NA	0.25	1	Susceptible	NA	8	GCA_000694515.1

^aInterpretive criteria are defined according to the European Committee on Antimicrobial Susceptibility Testing for colistin for "susceptible" and the Clinical and Laboratory Standards Institute for others; see text for details. MIN, minocycline; CST, colistin. Low concentration, individually ineffective concentration used in time-kill and RNA-Seq experiments. High concentration, individually effective concentration used in time-kill and RNA-Seq experiments; equivalent to MIC with the exception of minocycline for MGH 64 (see Fig. S2). NA, not applicable.

^bUsed in combination with polymyxin B nonapeptide (PMBN) at 16 μ g/mL.

^cUsed in combination with PMBN at 8 μ g/mL.

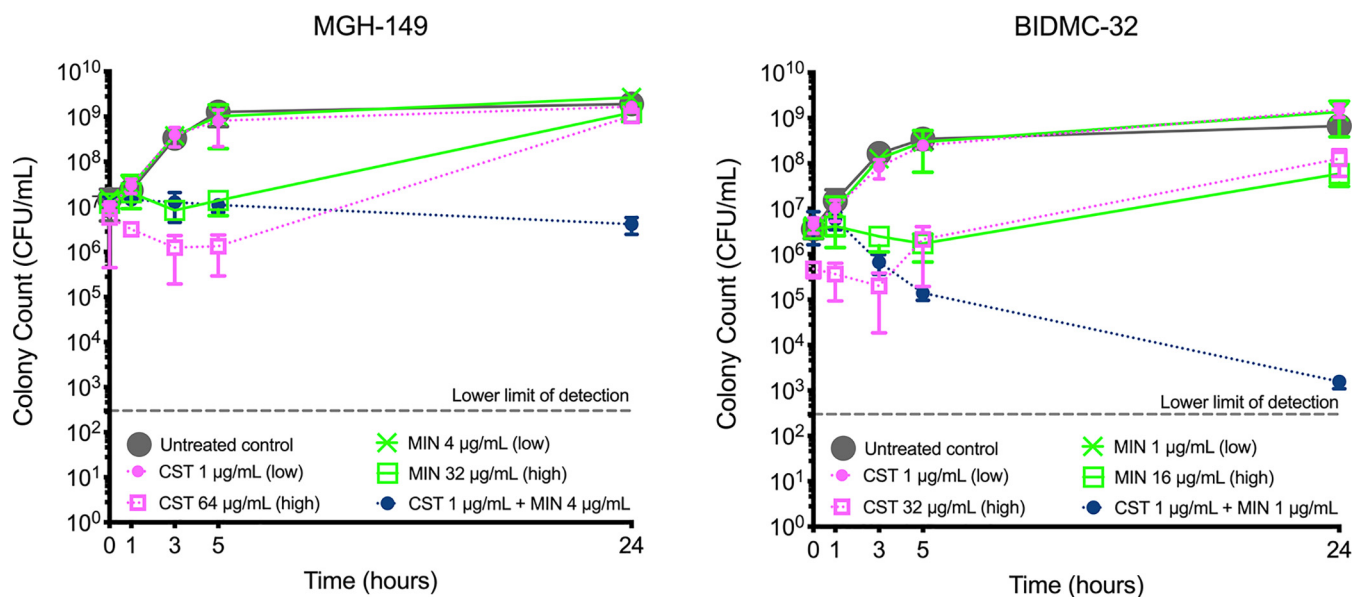


FIG 3 Time-kill curves of MGH-149 and BIDMC-32 treated with minocycline (MIN) and colistin (CST). Results represent the mean and standard deviation of 3 biological replicates. At 2 h, DNA was extracted from a culture set up under identical conditions in parallel with each replicate. “Low” and “high” refer to the low and high drug concentrations referenced in the text.

inhibitory concentration index [FIC_i]) among strains that were resistant to both colistin and minocycline but contained differing resistance-conferring mutations and belonged to different sequence types. MGH-149 contains the tetracycline-specific efflux pump, TetA, while both strains have mutations in the *ramR* gene, which encodes a repressor that downregulates expression of RamA, an AraC-family activator that increases AcrAB efflux pump expression and decreases porin expression, leading to decreased susceptibility to tetracycline antibiotics (Table 1) (11). Like most colistin-resistant *K. pneumoniae* strains, these isolates carried chromosomal mutations rather than plasmid-mediated *mcr* genes (25). Likely explaining its colistin resistance, MGH-149 lacks the *mgrB* gene, a negative regulator of the PhoP-PhoQ two-component system, which directs resistance-conferring modification of colistin’s target on lipopolysaccharide molecules (25, 26). BIDMC-32 lacks known resistance-conferring mutations in *mgrB* or other genes responsible for lipopolysaccharide modification in *K. pneumoniae*, including *phoPQ* and *pmrAB* (Table 1), but does carry a G to T transversion mutation 54 bases upstream of the start codon. This mutation, which is 27 bases downstream of the end of one proposed *mgrB* promoter region (26) and between the –35 and –10 sequences of a second proposed promoter region (27), may affect *mgrB* transcription, potentially through interference with proper promoter binding or activity.

For both strains, we generated synergy time-kill curves in parallel with growth of cells for RNA extraction to evaluate the phenotypic effect of the drugs on bacterial growth over time. Bacteria were treated with colistin and minocycline alone at an individually ineffective (low) concentration and with each drug alone at an effective (high) concentration, as well as with the two drugs in combination at low concentrations. Concentrations were selected based on results of checkerboard array susceptibility and synergy testing. An untreated control was included in each experiment. At 24 h, which is the standardized time point for evaluation of bactericidal and synergistic activity in time-kill studies, the combination of minocycline plus colistin was synergistic against both strains (i.e., resulted in a ≥ 2 log₁₀ reduction in CFU/mL at 24 h compared to the most active agent alone [28]) and was also bactericidal (i.e., resulted in a reduction of ≥ 3 log₁₀ CFU/mL at 24 h compared to the starting inoculum [29]) against BIDMC-32, but not against MGH-149 (Fig. 3).

In order to understand whether the combination of minocycline with PMBN, a polymyxin drug with outer membrane permeabilizing activity but no direct antibacterial

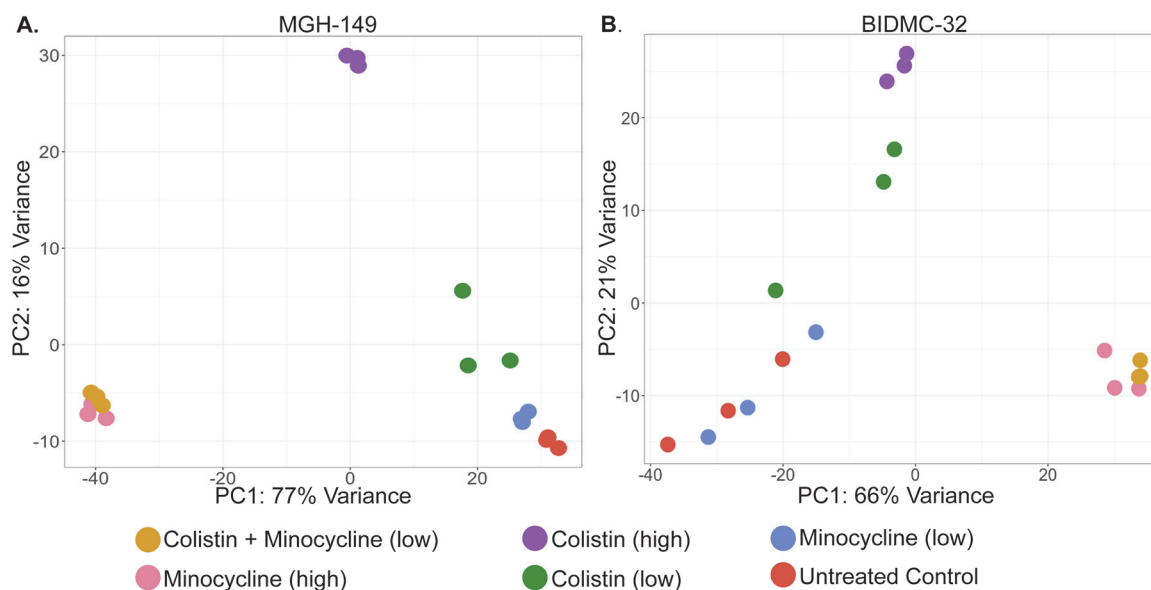


FIG 4 Principal-component analysis of the gene expression profiles for antibiotic-treated and untreated control *K. pneumoniae*. (A) PCA of MGH-149; (B) PCA of BIDMC-32. “Low” and “high” refer to the low and high drug concentrations referenced in the text.

activity, would show similar activity to that of colistin plus minocycline, we tested this combination against BIDMC-32 and against BIDMC-5, a strain that is classified as intermediate to minocycline and susceptible to colistin. These strains were selected in order to evaluate the effect of PMBN in combination against both a colistin-resistant and a colistin-susceptible strain that were otherwise similar in terms of sequence type and tetracycline resistance factors (Tables 1 and 2) and that both showed susceptibility to synergy of this combination in checkerboard array synergy testing. The combination was synergistic, although not bactericidal, against both strains in time-kill studies (Figure S1). Because we considered that the effects of minocycline and colistin against a resistant strain might be different than their effects against a susceptible isolate, we also tested each drug alone at an individually effective concentration against MGH-64, a representative clinical *K. pneumoniae* isolate that is susceptible to both of these drugs (Figure S2). In several instances, bacteria demonstrated regrowth at 24 h when treated with one or both drugs at the concentration identified as the MIC in initial susceptibility and checkerboard array synergy testing, which was performed using the digital dispensing method. The digital dispensing method is an adaptation of broth microdilution testing, and as MICs in the large volumes used in time-kill studies are often higher than MICs determined by broth microdilution testing (30), the observation of regrowth at 24 h is not unexpected.

The transcriptomic profile of the synergistic combination is highly similar to that of minocycline alone. We used RNA-Seq to profile the transcriptomes of colistin treatment alone, minocycline treatment alone, and the synergistic combination of colistin and minocycline. From each sample, an average of 11 million reads were generated, 79% of which, on average, aligned to a single reference genome, ATCC 700721/ MGH 78578 (GenBank accession number [NC_009648.1](https://www.ncbi.nlm.nih.gov/nuccore/NC_009648.1)), chosen for its similarity to MGH-149 and BIDMC-32 and allowing for cross-strain transcriptomic comparisons (20, 31, 32). Read counts were assigned to genes and other genomic features to generate the transcriptomic profile for each treatment. We performed unsupervised learning using principal-component analysis (PCA) on the transcriptomic profiles of each treatment in order to determine how the transcriptional responses to different drugs and drug combinations compared to one another. We found that, in both MGH-149 and BIDMC-32, the transcriptomic responses to the synergistic combination of minocycline and colistin at low concentrations clustered tightly with that of minocycline at high concentrations (Fig. 4). Reflective of the minimal effect individual drugs at low

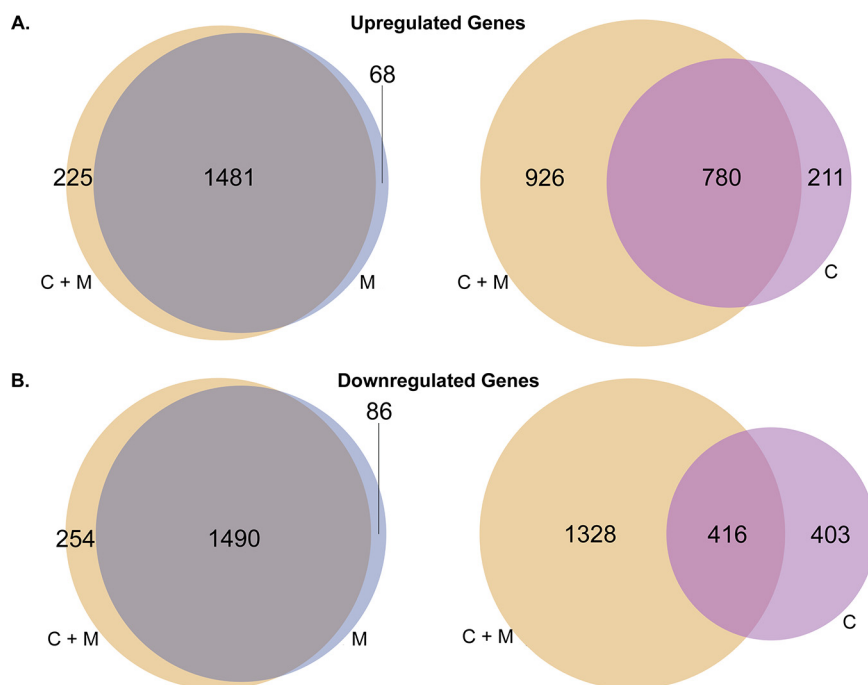


FIG 5 Shared upregulated and downregulated genes between colistin (high) treatment, minocycline (high) treatment and the combination of colistin and minocycline in MGH-149. (A) Upregulated and (B) downregulated differentially expressed genes in each treatment group in *K. pneumoniae* MGH-149 after treatment with colistin (purple), minocycline (blue), and the combination of colistin and minocycline (yellow). All comparisons are to the untreated control.

concentrations had on the growth of these resistant strains, each strain's transcriptomic response to exposure to low concentrations of either colistin or minocycline tended to cluster more closely with the untreated controls, while responses to colistin treatment at the high concentration tended to separate from both of these clusters by both principal components (Fig. 4). Principle components one and two accounted for 77% and 16% of the variance in MGH-149 and 66% and 21% of the variance in BIDMC-32, respectively. In both strains, high-dose minocycline treatment alone clusters tightly with the synergistic combination and away from the rest of the treatments along the first principle component.

Hierarchical clustering of the treatment groups based on gene expression again showed close clustering of the synergistic combination and minocycline at high concentrations, as well as shared patterns of coexpressed genes (Fig. S3A [MGH-149] and Fig. S3B [BIDMC-32]).

We next determined the differentially expressed genes for all antibiotic-treated samples compared to the untreated control using DESeq2 (33) (Tables S3 and S4). In both strains, the synergistic combination yielded the highest number of differentially expressed genes, followed by minocycline treatment at high concentrations. For both strains, the majority of upregulated genes (87% MGH-149, 88% BIDMC-32) and downregulated genes (86% MGH-149, 87% BIDMC-32) in the synergistic combination were also upregulated and downregulated, respectively, at high minocycline concentrations (Fig. 5 and 6). There were fewer overlaps between differentially expressed genes at high colistin concentrations and the synergistic combination; less than half (46% MGH-149, 13% BIDMC-32) of upregulated genes and less than a quarter (24% MGH-149, 18% BIDMC-32) of downregulated genes in the synergistic combination were also upregulated and downregulated, respectively, at high colistin concentrations (Fig. 5 and 6). Similar sets of Gene Ontology (GO) terms were also enriched in the differentially expressed genes of both strains following treatment with minocycline and the

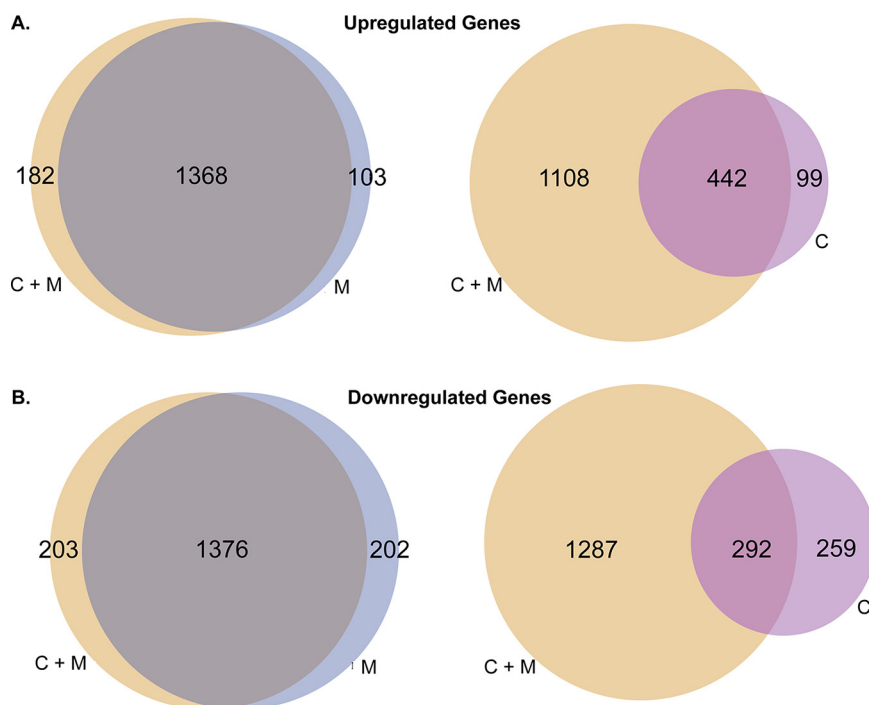


FIG 6 Shared upregulated and downregulated genes between colistin (high) treatment, minocycline (high) treatment, and the combination of colistin and minocycline in BIDMC-32. (A) Upregulated and (B) downregulated differentially expressed genes in each treatment group in *K. pneumoniae* BIDMC-32 after treatment with colistin (purple), minocycline (blue), and the combination of colistin and minocycline (yellow). All comparisons are to the untreated control.

synergistic combination, consistent with the high degree of gene expression overlap (Fig. S4A to D).

GO-term enrichment of the downregulated genes in both the synergistic combination and high-concentration minocycline treatment was characterized by terms related to metabolic and biosynthetic processes. In contrast, GO-term enrichment of downregulated genes in high-concentration colistin treatment was dominated by ion transport functions, including transmembrane transport, as well as membrane-related terms (Fig. S4B and S4D). These different enrichment patterns may reflect the inhibition of protein synthesis by minocycline, on the one hand, and the impairment of outer membrane integrity by colistin on the other. GO-term enrichment of upregulated genes demonstrated enrichment of genes involved in biosynthesis and metabolism for all treatment conditions, suggesting that upregulated genes, at least under the conditions examined here, may be less reflective of specific antibiotic effects and, instead, reflect a more generalized stress response (Fig. S4 and S6).

Genes involved in polymyxin resistance show significant differential gene expression. Most colistin resistance in *K. pneumoniae* occurs via the addition of moieties including L-ara4N to lipid A. This modification decreases the net negative charge of lipid A, reducing binding of polymyxin antibiotics such as colistin (7). Treatment of polymyxin-susceptible *K. pneumoniae* with polymyxin B, a drug closely related to colistin, has previously been observed to increase expression of some genes in the *arnBCADTEF* operon (also known as *pmrHFIJKLM* or *pbgPE*) (18, 34, 35), which encodes enzymes responsible for this lipid A modification (Fig. 7A). We investigated the effects of colistin and the colistin-minocycline combination on expression of these genes in colistin-resistant strains. When colistin-resistant MGH-149 and BIDMC-32 were treated with high-concentration colistin, genes in the *arnBCADTEF* operon pathway were highly upregulated, whereas upon treatment with the synergistic combination, these genes were significantly downregulated, as they also were upon treatment with high-concentration minocycline alone (Fig. 7B). In contrast, genes in the *arnBCADTEF* operon

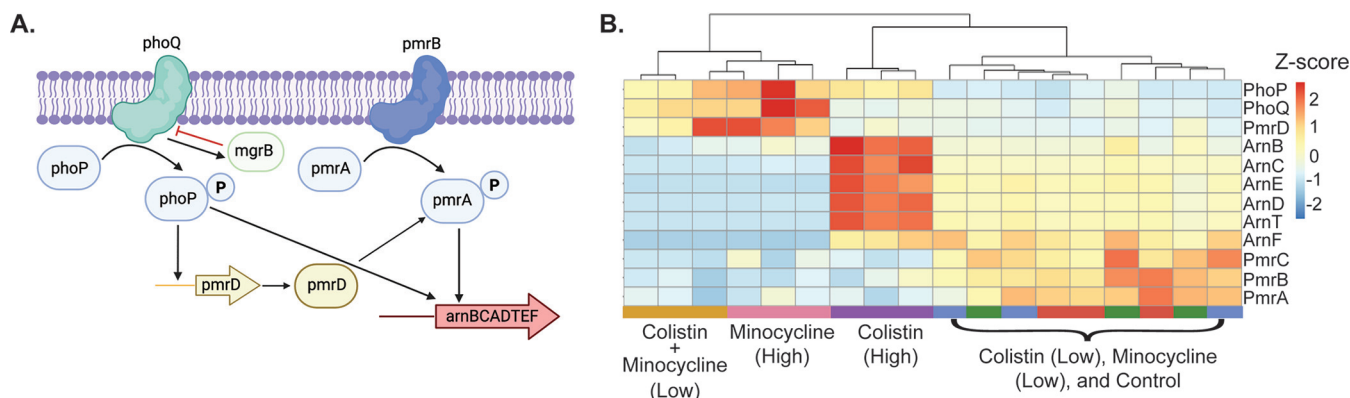


FIG 7 Differential gene expression in the *arnBCADTEF* operon and other genes involved in polymyxin resistance. (A) Schematic of the PhoPQ and PmrAB two-component systems and how they control expression of the *arn* operon. Activation of *arnBCADTEF* mediated through the PmrD relay of PmrAB signaling, as well as direct activation by PhoP have been described (35, 37). (B) Heatmap of gene expression of the pathway in MGH-149 using normalized CPMs showing clustering of biological replicates. Expression was scaled using Z-score normalization prior to clustering, with red representing high expression and blue representing low expression. “Low” and “high” refer to the low and high drug concentrations referenced in the text.

pathway were not upregulated during exposure to colistin in a colistin-susceptible isolate (Fig. S5). Taken together, these findings suggest that the subinhibitory permeabilizing activity of low-concentration colistin, as part of combination treatment with minocycline, does not induce pathways promoting colistin resistance, in contrast to treatment with high-concentration colistin alone in colistin-resistant bacteria. We also examined the expression of *pmrD*, which encodes a protein that responds to PhoP signaling by stimulating the two-component system PmrAB, which in turn upregulates the *arnBCADTEF* operon (36). PmrD-mediated activation of the *arnBCADTEF* operon is well described in *Salmonella* (35) but appears to play a more limited role in *K. pneumoniae*, where direct PhoP activation predominates (27, 37). In keeping with these findings, we did not observe increased expression of *pmrD* on treatment with high concentrations of colistin, suggesting direct activation of *arnBCADTEF* by PhoP (Fig. 7). Conversely, *pmrD* was upregulated to various degrees during treatment with minocycline and with the colistin plus minocycline combination, but without associated upregulation of *arnBCADTEF*.

The synergistic combination downregulates cell envelope biogenesis. Neither colistin nor minocycline are generally understood to act on synthesis of peptidoglycan in the cell envelope. However, the combination of polymyxin B with chloramphenicol (an antibiotic which, like minocycline, targets protein synthesis in the ribosome) was recently shown to downregulate genes involved in peptidoglycan synthesis (18). To see if the combination of minocycline and colistin would have a similar effect, we evaluated the expression of genes in these pathways. The synergistic combination and high-concentration minocycline alone, but not high-concentration colistin alone, significantly downregulated the *murB*, *murC*, *murD*, *murE*, *murI*, and *murJ* genes involved in peptidoglycan synthesis. (Fig. S6). This effect suggests the possibility that inhibition of cell envelope biosynthesis may play an unexpected role in the activity of minocycline and the combination, perhaps as a general result of inhibition of protein synthesis; additional work would be required to determine to what degree this effect might be specific to tetracyclines and/or protein synthesis inhibitor drugs in general.

The combination of PMBN and minocycline also has a transcriptomic profile similar to that of minocycline alone. We observed that PMBN was also synergistic with minocycline against both colistin-resistant and colistin-susceptible isolates. In antibiotic combinations, PMBN has theoretical therapeutic advantages over colistin in terms of potential reduced toxicity, and PMBN analogs have been explored for clinical use as antibiotic potentiators (38, 39). We were therefore interested in assessing how similar the transcriptional response to the combination of PMBN and minocycline was to the combination of colistin and minocycline. (No individually active concentration was tested for PMBN alone, as it does not have antimicrobial activity when used alone.)

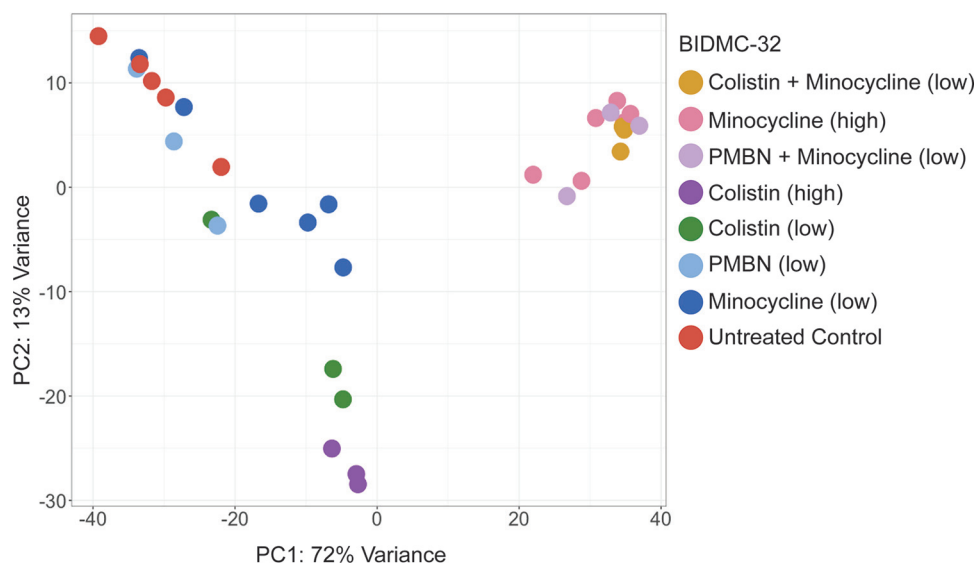


FIG 8 Principal-component analysis of the gene expression profiles for antibiotic-treated and untreated control *K. pneumoniae* strain BIDMC-32. “Low” and “high” refer to the low and high drug concentrations referenced in the text. PMBN does not inhibit bacterial growth at any concentration tested (it does not have an MIC) and therefore was tested both alone and in combination with minocycline at its FIC (“low”).

PCA showed clustering of the PMBN and minocycline combination with that of colistin and minocycline, as well as with high-concentration minocycline alone, suggesting the possibility that there may be similar mechanisms for all three treatment conditions (Fig. 8).

DISCUSSION

Polymyxins, including colistin, have long been recognized as outer membrane-disrupting agents that facilitate uptake of hydrophobic antibiotics that are normally excluded from the interior of Gram-negative cells as a result of their inability to cross the outer membrane (40). When colistin-susceptible bacteria are treated with colistin at concentrations above the MIC, this outer membrane permeabilization effect is combined with cytoplasmic membrane disruption, resulting in cell lysis and death. Recently, studies describing synergistic activity of colistin-containing antibiotic combinations against colistin-resistant bacteria have provided evidence that colistin retains outer membrane permeabilizing activity against colistin-resistant bacteria even at concentrations below the MIC, despite its absence of lytic activity or growth inhibition at these concentrations (9, 41). An analogous phenomenon of isolated permeabilization occurs when bacteria are treated with PMBN, which retains the outer membrane permeabilizing effect but not the cytoplasmic membrane-disrupting effect of its parent compound (42). In the results presented here, we observed a striking similarity between the transcriptomic profiles of colistin- and minocycline-resistant *K. pneumoniae* isolates treated with a combination of colistin and minocycline at individually subinhibitory concentrations and the profiles of those same isolates treated with minocycline alone and with PMBN plus minocycline. These findings support the hypothesis that the synergistic activity of the colistin plus minocycline combination involves sublethal cell envelope disruption by colistin, which permits increased intracellular accumulation of minocycline. Tetracycline antibiotics can enter Gram-negative cells either through porin channels or by diffusion through the outer membrane lipid bilayer (43), with outer membrane diffusion playing a larger role for hydrophobic tetracycline derivatives such as minocycline (44). It is thus logical that increased permeability of the outer membrane would have a marked effect on minocycline entry into the cell and

that an increased rate of entry could overcome drug efflux (45), which is the primary mechanism of minocycline resistance in the strains evaluated here.

While the explanation for the decoupling of outer membrane permeabilization and cell lysis in colistin-resistant bacteria is not fully understood (46), it may involve the presence of lipid A molecules at the cytoplasmic membrane that undergo resistance-conferring modifications at a higher rate relative to the outer membrane, leading to decreased vulnerability of the cytoplasmic membrane to the effect of colistin (47, 48). Loss of the fatty acid tail in PMBN results in a phenotypically similar effect to the impaired polypeptide head binding of colistin in colistin-resistant bacteria, yet the exact explanation for the loss of lytic activity in PMBN also remains incompletely elucidated. It has been proposed that self-promoted uptake of colistin across the outer membrane involves insertion of the fatty acid tail into the outer membrane (5). Lacking this tail, PMBN would be unable to reach the cytoplasmic membrane, while its permeabilizing effect at the outer membrane would remain unaffected. Consistent with this hypothesis, PMBN has been shown to cause leakage of periplasmic but not cytoplasmic proteins (49). One report describes loss of K⁺, uracil, and amino acids across the cytoplasmic membrane during treatment with PMBN, but the rate of loss was less than during treatment with polymyxin B and was not associated with bacterial killing (6). Interestingly, PMBN treatment causes less morphological outer membrane damage than polymyxin B, suggesting that there may in fact also be differences between PMBN and intact polymyxin compounds in terms of outer membrane disruption (49). We observed bacteriostatic synergistic activity against both colistin-resistant and colistin-susceptible strains when PMBN was combined with minocycline (Fig. S1) (in contrast to bactericidal activity of colistin and minocycline against one of the same strains), and noted that treatment of the colistin-resistant strain BIDMC-32 with minocycline and PMBN resulted in a transcriptomic profile that clustered tightly with that of the combination of minocycline and colistin (Fig. 8). These observations do not fully disentangle the relative roles of the polypeptide head and fatty acid tail in the activity of polymyxins and polymyxin derivatives at the outer membrane and cytoplasmic membrane. However, they do provide further evidence of the highly similar inhibitory process effected by PMBN and, in colistin-resistant bacteria, by colistin, when combined with intracellularly active antibiotics.

We observed that genes in the *arnBCADTEF* operon were upregulated during treatment with colistin alone and downregulated during treatment with minocycline alone or the combination of colistin and minocycline. A similar pattern was observed by Abdul Rahim and colleagues in a polymyxin B-susceptible *K. pneumoniae* isolate treated with polymyxin B, chloramphenicol (a protein synthesis inhibitor antibiotic), and the combination (18). The *arnBCADTEF* operon mediates production of 4-amino-4-deoxy-L-arabinose (L-Ara4N) and addition of this molecule to lipid A, which causes a reduction in the negative charge of lipid A and a resultant inability of colistin to bind to this target (7). Modification of lipid A by L-Ara4N is the most common mechanism of colistin resistance in *K. pneumoniae* (50) and the expected mechanism in strains MGH-149 (as a result of loss of the *mgrB* repressor gene) and BIDMC-32 (possibly through a point mutation located between the promoter and start codon of the *mgrB* gene). The PhoP/PhoQ two-component system, which operates upstream of expression of the *arnBCADTEF* operon, is known to be responsive to antimicrobial peptides (51) and has been shown to be upregulated by polymyxin B exposure in *Pseudomonas aeruginosa* (52), so it is possible PhoP/PhoQ is activated in response to colistin, resulting in downstream upregulation of the *arnBCADTEF* operon in a feed-forward pattern of colistin-responsive colistin resistance. (We note that neither *phoP/phoQ* nor *pmrA/pmrB* were upregulated during colistin treatment, but we would not necessarily expect activation of these two-component systems to result in changes in their gene expression). We did not observe upregulation of the *arnBCADTEF* operon in response to colistin exposure in the colistin-susceptible strain MGH-64 (Fig. S5). Upregulation of the *arnBCADTEF* operon did not occur during exposure to minocycline alone or to the synergistic combination of minocycline and colistin, suggesting that the subinhibitory action of low concentrations of colistin on colistin-resistant

bacteria may not induce its own resistance. This finding, along with the observation that the combination, but not either drug alone, prevented regrowth at 24 h in the time-kill experiments, suggests that the combination may be more resilient against the emergence of bacterial resistance or tolerance.

The development of novel antimicrobials over the past several decades has failed to keep pace with the emergence of multidrug resistance, particularly among Gram-negative bacteria (53). Colistin has traditionally been considered a drug of last resort for treatment of highly resistant Gram-negative pathogens, but it is not a useful treatment option for the increasing number of colistin-resistant isolates (54), and its narrow therapeutic window limits its clinical utility in treating even colistin-susceptible strains (55). Synergistic combinations of individually ineffective drugs, as evaluated here, offer potential therapeutic alternatives that do not depend on the development of new antibacterial agents. Indeed, a PMBN-like compound with outer membrane permeabilizing activity has been evaluated as an antibiotic potentiator against multidrug-resistant Gram-negative pathogens and has undergone phase I investigation (39, 56). Although efficacy studies in human subjects will ultimately be required to assess the clinical efficacy of such combinations, *in vitro* investigations such as we present here can inform such studies by helping to elucidate the mechanism of action and indicating plausible dosing regimens.

Transcriptomic studies can provide insight into a wide range of cellular processes by comparing large, systematically acquired data sets, but they also possess certain intrinsic limitations. Although we can identify genes and gene pathways that are up- or downregulated, we cannot, for example, quantify translation or protein levels. However, identifying significantly differentially expressed genes can help shed light on partially understood processes and allows us to prioritize pathways for further evaluation using complementary techniques.

We present here a novel use of this promising technology to further our understanding of antimicrobial combination therapy for treatment of some of the most highly drug-resistant pathogens identified to date. Many antibiotics still in common use, including tetracyclines and polymyxins, as well as β -lactam drugs (e.g., penicillin), were discovered and entered clinical use long before the scientific tools necessary to elucidate their mechanisms of action had been developed. As a result, much still remains unknown about the spectrum of effects that each of these compounds exerts on bacteria, and RNA-Seq analysis, as we have demonstrated here, can provide a valuable tool for enhancing our understanding of these drugs.

MATERIALS AND METHODS

Bacterial strains. *Klebsiella pneumoniae* strains were obtained from the carbapenem-resistant *Enterobacterales* genome initiative at the Broad Institute (Cambridge, MA; 213 strains) (20) and the U.S. Food and Drug Administration (FDA)-CDC Antimicrobial Resistance Isolate Bank (Atlanta, GA; 6 strains). A full list of strains is included in Table S1. *Escherichia coli* ATCC 25922 was obtained from the American Type Culture Collection (Manassas, VA). All strains were colony purified, minimally passaged, and stored at 80°C in tryptic soy broth with 50% glycerol (Sigma-Aldrich, St. Louis, MO) until the time of use.

Antibiotics. Colistin sulfate was obtained from Santa Cruz Biotechnology (Santa Cruz, CA), and minocycline hydrochloride was obtained from Chem-Impex International (Wood Dale, IL). Antibiotic stock solutions for time-kill studies and for growth of bacteria for RNA extraction were prepared in water; stock solutions used for the digital dispensing method were prepared in water with 0.3% polysorbate 20 (P-20; Sigma-Aldrich, St. Louis, MO) as required by the D300 digital dispenser instrument (HP, Inc., Palo Alto, CA) for proper fluid handling. All antibiotic stock solutions were quality control tested with *E. coli* ATCC 25922 by standard a broth microdilution technique using the direct colony suspension method (57) or the digital dispensing method (for stocks to be used for checkerboard arrays) prior to use. Antimicrobial solutions were stored as aliquots at 20°C and were discarded after a single use.

Checkerboard array synergy testing and MIC determination. To create checkerboard arrays, serial 2-fold dilutions of colistin (concentration range, 0.016 to 16 $\mu\text{g}/\text{mL}$) and minocycline (concentration range, 0.008 to 32 $\mu\text{g}/\text{mL}$) were dispensed in orthogonal titrations by the D300 instrument using the digital dispensing method previously developed by our group (19, 21). Bacterial inocula were prepared by suspending colonies in cation-adjusted Mueller-Hinton broth (CAMHB; BD Diagnostics, Franklin Lakes, NJ) and diluting to a final concentration of 5×10^5 CFU/mL. Antimicrobial stocks were dispensed in appropriate volumes into empty, flat-bottomed, untreated 384-well polystyrene plates (Greiner Bio-One, Monroe, NC) by the D300. Immediately after addition of antimicrobials, the wells were inoculated

with 50 μ L of bacterial suspension, and the plates were incubated for 16 to 20 h at 35°C in ambient air. After incubation, bacterial growth was quantified by measurement of optical density at 600 nm (OD_{600}) using an Infinite M1000 Pro microplate reader (Tecan, Morrisville, NC). An OD_{600} reading of 0.07 or greater (concordant with visual growth assessment) was considered indicative of bacterial growth. MICs for each antibiotic were determined from wells in the array containing only that drug. Isolates were considered susceptible, intermediate, or resistant according to CLSI breakpoint tables (58), with the exception of the classification of susceptible for colistin, as CLSI does not have a “susceptible” category for colistin for *Enterobacteriales*; isolates with an MIC of $\leq 2 \mu$ g/mL are classified as “intermediate” to reflect colistin’s limited clinical efficacy. For clarity in the manuscript, we used the current European Committee on Antimicrobial Susceptibility Testing (EUCAST) interpretive criteria for colistin for *Enterobacteriales*, which classifies isolates with an MIC of ≤ 2 as susceptible (59). For each concentration of each drug, the well in which growth was inhibited at the lowest concentration of the other drug was identified. For each of these wells, the fractional inhibitory concentration (FIC) for each antibiotic was calculated by dividing the concentration of the antibiotic in that well by the MIC of the antibiotic. The fractional inhibitory concentration (FIC) index (FIC_i) for each well was then determined by summing the FICs of the two drugs. If the MIC of an antibiotic was off scale, the highest concentration tested was assigned an FIC of 0.5 to permit FIC_i calculation. When the minimum FIC_i in a synergy grid was ≤ 0.5 , the combination was considered synergistic for that bacterial isolate, and when the maximum FIC_i was >4.0 , the combination was considered antagonistic. When all FIC_i values were intermediate, the combination was considered to have no interaction. In cases where a single grid included both synergistic and antagonistic FIC_i values, the combination was considered to have a mixed effect.

Identification of antibiotic resistance genes. Genes and gene mutations known to confer resistance to colistin and tetracyclines were identified using the Resistance Gene Identifier tool (RGI 5.2.0) in the Comprehensive Antibiotic Resistance Database (CARD 3.1.4; <https://card.mcmaster.ca/home>) (60) with the parameters “perfect and strict hits only” and “include nudge $\geq 95\%$ identity loose hits to strict,” as well as ResFinder 4.1 (<https://cge.cbs.dtu.dk/services/ResFinder/>) (61–63) with the following parameters: for chromosomal point mutations, 98% threshold for %ID, 80% minimum length, unknown mutations included; for acquired antimicrobial resistance genes, colistin and tetracycline, 98% threshold for % ID, 80% minimum length; for species, *Klebsiella*. In addition, individual gene sequences from strains discussed in this paper were compared to reference sequences using the Basic Local Alignment Search Tool (BLAST) program from the National Center for Biotechnology Information (<https://blast.ncbi.nlm.nih.gov/Blast.cgi>) and were further analyzed using SnapGene 5.3.2 (San Diego, CA). Insertion sequences were evaluated using ISfinder (<http://www.is-biotoul.fr>) (64).

Growth conditions for RNA extraction. Time-kill synergy studies and RNA extraction for RNA-Seq were performed using the following *K. pneumoniae* isolates and treatment conditions (Table 2): BIDMC-32, exposed to minocycline and colistin and to minocycline and polymyxin B nonapeptide, separately and in combination, MGH-149, exposed to minocycline and colistin, separately and in combination, BIDMC-5, exposed to minocycline and polymyxin B nonapeptide, separately and in combination, and MGH-64, exposed to minocycline and colistin separately. Antibiotic concentrations under each condition were selected based on results of checkerboard array synergy testing, with final concentrations adjusted as necessary, based on preliminary time-kill experiments, to account for expected differences in MIC and FIC concentrations between the microdilution volumes used in checkerboard array experiments (50 μ L per reaction) and in time-kill experiments (15 mL per reaction). Antibiotic stocks were prepared in water and constituted a volume of $\leq 3.2\%$ of the total volume of the culture; because the carrier volume was small and consisted only of water, blank carrier liquid was not added to untreated controls. For each antibiotic/bacterial strain condition, two identical culture tubes were prepared in parallel from the same starting inoculum, with one used for the time-kill study and one used for RNA extraction. All studies were performed with three biological replicates. Antibiotic stocks were prepared as described above and diluted in 15 mL of CAMHB in 25- by 150-mm glass round-bottom tubes to the desired starting concentrations. An initial starting inoculum was prepared by adding 250 μ L of a 0.5 McFarland suspension of colonies from an overnight plate to 12.5 mL of CAMHB and incubating the mixture on a shaker in ambient air at 35°C until the suspension reached log-phase growth (approximately 4 h). The culture was then adjusted to the turbidity of a 1.0 McFarland standard in CAMHB, and 0.75 mL of this suspension was added to each of the tubes containing antimicrobial solutions for a final starting inoculum of $\sim 5 \times 10^6$ CFU/mL. An untreated control and a negative-control tube were prepared in parallel with each experiment. Cultures were incubated on a shaker in ambient air at 35°C. For RNA extraction, one set of tubes was removed from the incubator at 2 h. The contents of each tube were spun at $2,000 \times g$ for 20 min at 4°C. The supernatant was removed, and the pellet was resuspended in 0.5 mL of TRIzol reagent (Invitrogen, Waltham, MA), incubated at room temperature for 5 min, and then frozen at -80°C until the time of RNA extraction. For the time-kill study, aliquots from each culture tube from the second set of tubes were removed for colony enumeration at 0, 1, 3.5, and 24 h (MGH-64) and at 0, 1, 3, 5, and 24 h (other strains). To perform colony counts, a 10-fold dilution series was prepared in 0.9% sodium chloride. A 10 μ L drop from each dilution was transferred to a Mueller-Hinton plate (Thermo Fisher, Waltham, MA) and incubated overnight in ambient air at 35°C (65). For countable drops (drops containing 3 to 30 colonies), the cell density of the sample was calculated; if more than one dilution for a given sample was countable, the cell density of the two dilutions was averaged. If no drops were countable, the counts for consecutive drops above and below the countable range were averaged. The lower limit of detection was 300 CFU/mL.

RNA extraction. Cell pellets resuspended in 0.5 mL TRIzol reagent (Thermo Fisher Scientific) were transferred to 2-mL FastPrep tubes (MP Biomedicals) containing 0.1 mm zirconia/silica beads (BioSpec

Products) and bead-beaten for 90 s at 10 m/s speed using the FastPrep-24 5G instrument (MP Biomedicals). After addition of 200 μ L chloroform, each sample tube was mixed thoroughly by inversion, incubated for 3 min at room temperature, and spun down for 15 min at 4°C. The aqueous phase was mixed with an equal volume of 100% ethanol and transferred to a Direct-zol spin plate (Zymo Research), and RNA was extracted according to the Direct-zol protocol (Zymo Research).

Generation of RNA-Seq data. Illumina cDNA libraries were generated using a modified version of the RNAtag-seq protocol (66, 67). Briefly, 500 ng to 1 μ g of total RNA was fragmented, depleted of genomic DNA, dephosphorylated, and ligated to DNA adapters carrying 5'-AN₈-3' barcodes of known sequence with a 5' phosphate and a 3' blocking group. Barcoded RNAs were pooled and depleted of rRNA using the RiboZero rRNA depletion kit (Epicentre). Pools of barcoded RNAs were converted to Illumina cDNA libraries in 2 main steps: (i) reverse transcription of the RNA using a primer designed to the constant region of the barcoded adaptor with addition of an adapter to the 3' end of the cDNA by template switching using SMARTScribe (Clontech) as previously described (3) and (ii) PCR amplification using primers whose 5' ends target the constant regions of the 3' or 5' adaptors and whose 3' ends contain the full Illumina P5 or P7 sequences. cDNA libraries were sequenced to generate paired-end reads.

Analysis of RNA-Seq data. Sequencing reads from each sample in a pool were demultiplexed based on their associated barcode sequence using custom scripts (https://github.com/broadinstitute/split_merge_pl). Up to 1 mismatch in the barcode was allowed, provided it did not make assignment of the read to a different barcode possible. Barcode sequences were removed from the first read, as were terminal Gs from the second read that may have been added by SMARTScribe during template switching. Reads were aligned to ATCC 700721/MGH 78578 (GenBank accession number [NC_009648.1](https://.ncbi.nlm.nih.gov/nuccore/NC_009648.1)), a multi-drug-resistant reference strain originally isolated from the sputum of a patient (20, 31, 32) using the Burrows-Wheeler Aligner (BWA) (68), and read counts were assigned to genes and other genomic features using custom scripts (<https://github.com/broadinstitute/BactRNASeqCount>). Read counts were used as input to DESeq2 (release 3.12) to build a DESeq data set (33). Differential gene expression analysis was performed using DESeq2 default settings. In order to check for batch effects, principal-component analysis (PCA) was performed on biological replicates after variance-stabilizing transformation to obtain transformed, normalized counts. Differentially expressed genes were determined between each treatment group and the untreated control. Genes were determined as differentially expressed using a threshold of $P < 0.05$ and a false-discovery rate (FDR) of 5%, standard settings in DESeq2. Differential gene expression analysis was also performed using edgeR (v3.32.1) (69, 70), obtaining very similar results to DESeq2. edgeR was used to calculate counts per million (CPMs), for each gene, which were used for the unsupervised clustering and heatmap generation.

Data analysis. Statistical analysis was performed using R (v4.0.2; R Foundation, Vienna, Austria). The chi-square test was used for comparison of proportions.

SUPPLEMENTAL MATERIAL

Supplemental material is available online only.

SUPPLEMENTAL FILE 1, XLSX file, 0.1 MB.

SUPPLEMENTAL FILE 2, XLSX file, 0.04 MB.

SUPPLEMENTAL FILE 3, XLSX file, 0.2 MB.

SUPPLEMENTAL FILE 4, XLSX file, 0.2 MB.

SUPPLEMENTAL FILE 5, PDF file, 2.1 MB.

ACKNOWLEDGMENTS

RNA-Seq libraries were constructed and sequenced at the Broad Institute of MIT and Harvard by the Microbial 'Omics Core and Genomics Platform, respectively. The Microbial 'Omics Core also provided guidance on experimental design and conducted preliminary analysis for all RNA-Seq data.

We thank Abigail Manson, Roby Bhattacharyya, Noam Shoresh, and Alejandro Pironti for their input and suggestions.

T.B.-K. was supported by a Eunice Kennedy Shriver National Institute of Child Health and Human Development pediatric infectious diseases research training grant (T32HD055148), a National Institute of Allergy and Infectious Diseases (NIAID) training grant (T32AI007061), a Boston Children's Hospital Office of Faculty Development Faculty Career Development fellowship, and a NIAID career development award (1K08AI132716). A.G. was supported by the Jane Coffin Childs Memorial Fund for Medical Research. This work was also funded in part with federal funds from the National Institute of Allergy and Infectious Diseases, National Institutes of Health, Department of Health and Human Services, under grant number U19AI110818 to the Broad Institute.

The HP D300 digital dispenser and TECAN M1000 used in experiments were provided by TECAN (Morrisville, NC). TECAN had no role in study design, data collection/interpretation,

manuscript preparation, or the decision to publish. Figures 1, 2, and 7A were created with BioRender.

REFERENCES

- Ordooei Javan A, Shokouhi S, Sahraei Z. 2015. A review on colistin nephrotoxicity. *Eur J Clin Pharmacol* 71:801–810. <https://doi.org/10.1007/s00228-015-1865-4>.
- Falagas ME, Kasiakou SK. 2005. Colistin: the revival of polymyxins for the management of multidrug-resistant gram-negative bacterial infections. *Clin Infect Dis* 40:1333–1341. <https://doi.org/10.1086/429323>.
- Nation RL, Li J. 2009. Colistin in the 21st century. *Curr Opin Infect Dis* 22:535–543. <https://doi.org/10.1097/QCO.0b013e328332e672>.
- Ah Y-M, Kim A-J, Lee J-Y. 2014. Colistin resistance in *Klebsiella pneumoniae*. *Int J Antimicrob Agents* 44:8–15. <https://doi.org/10.1016/j.ijantimicag.2014.02.016>.
- Storm DR, Rosenthal KS, Swanson PE. 1977. Polymyxin and related peptide antibiotics. *Annu Rev Biochem* 46:723–763. <https://doi.org/10.1146/annurev.bi.46.070177.003451>.
- Dixon RA, Chopra I. 1986. Polymyxin B and polymyxin B nonapeptide alter cytoplasmic membrane permeability in *Escherichia coli*. *J Antimicrob Chemother* 18:557–563. <https://doi.org/10.1093/jac/18.5.557>.
- Olaitan AO, Morand S, Rolain J-M. 2014. Mechanisms of polymyxin resistance: acquired and intrinsic resistance in bacteria. *Front Microbiol* 5:643. <https://doi.org/10.3389/fmicb.2014.00643>.
- Odds FC. 2003. Synergy, antagonism, and what the checkerboard puts between them. *J Antimicrob Chemother* 52:1. <https://doi.org/10.1093/jac/dkg301>.
- Brennan-Krohn T, Pironti A, Kirby JE. 2018. Synergistic activity of colistin-containing combinations against colistin-resistant Enterobacteriaceae. *Antimicrob Agents Chemother* 62:e00873-18. <https://doi.org/10.1128/AAC.00873-18>.
- Brennan-Krohn T, Kirby JE. 2019. Synergistic combinations and repurposed antibiotics active against the pandrug-resistant *Klebsiella pneumoniae* Nevada strain. *Antimicrob Agents Chemother* 63:e01374-19. <https://doi.org/10.1128/AAC.01374-19>.
- Grossman TH. 2016. Tetracycline antibiotics and resistance. *Cold Spring Harb Perspect Med* 6:a025387. <https://doi.org/10.1101/cshperspect.a025387>.
- Vaara M, Vaara T. 1983. Polycations sensitize enteric bacteria to antibiotics. *Antimicrob Agents Chemother* 24:107–113. <https://doi.org/10.1128/AAC.24.1.107>.
- Vaara M, Vaara T. 1983. Sensitization of Gram-negative bacteria to antibiotics and complement by a nontoxic oligopeptide. *Nature* 303:526–528. <https://doi.org/10.1038/303526a0>.
- Vaara M, Vaara T. 1983. Polycations as outer membrane-disorganizing agents. *Antimicrob Agents Chemother* 24:114–122. <https://doi.org/10.1128/AAC.24.1.114>.
- SEQC/MAQC-III Consortium. 2014. A comprehensive assessment of RNA-seq accuracy, reproducibility and information content by the Sequencing Quality Control Consortium. *Nat Biotechnol* 32:903–914. <https://doi.org/10.1038/nbt.2957>.
- Croucher NJ, Thomson NR. 2010. Studying bacterial transcriptomes using RNA-seq. *Curr Opin Microbiol* 13:619–624. <https://doi.org/10.1016/j.mib.2010.09.009>.
- Ramos PIP, Custódio MGF, Quispe Saji GDR, Cardoso T, da Silva GL, Braun G, Martins WMBS, Girardello R, de Vasconcelos ATR, Fernández E, Gales AC, Nicolás MF. 2016. The polymyxin B-induced transcriptomic response of a clinical, multidrug-resistant *Klebsiella pneumoniae* involves multiple regulatory elements and intracellular targets. *BMC Genomics* 17:737. <https://doi.org/10.1186/s12864-016-3070-y>.
- Abdul Rahim N, Cheah S-E, Johnson MD, Zhu Y, Yu HH, Sidjabat HE, Butler MS, Cooper MA, Fu J, Paterson DL, Nation RL, Boyce JD, Bergen PJ, Velkov T, Li J. 2020. Transcriptomic responses of a New Delhi metallo- β -lactamase-producing *Klebsiella pneumoniae* isolate to the combination of polymyxin B and chloramphenicol. *Int J Antimicrob Agents* 56:106061. <https://doi.org/10.1016/j.ijantimicag.2020.106061>.
- Brennan-Krohn T, Truelson KA, Smith KP, Kirby JE. 2017. Screening for synergistic activity of antimicrobial combinations against carbapenem-resistant Enterobacteriaceae using inkjet printer-based technology. *J Antimicrob Chemother* 72:2775–2781. <https://doi.org/10.1093/jac/dkx241>.
- Cerqueira GC, Earl AM, Ernst CM, Grad YH, Dekker JP, Feldgarden M, Chapman SB, Reis-Cunha JL, Shea TP, Young S, Zeng Q, Delaney ML, Kim D, Peterson EM, O'Brien TF, Ferraro MJ, Hooper DC, Huang SS, Kirby JE, Onderdonk AB, Birren BW, Hung DT, Cosimi LA, Wortman JR, Murphy CI, Hanage WP. 2017. Multi-institute analysis of carbapenem resistance reveals remarkable diversity, unexplained mechanisms, and limited clonal outbreaks. *Proc Natl Acad Sci U S A* 114:1135–1140. <https://doi.org/10.1073/pnas.1616248114>.
- Smith KP, Kirby JE. 2016. Verification of an automated, digital dispensing platform for at-will broth microdilution-based antimicrobial susceptibility testing. *J Clin Microbiol* 54:2288–2293. <https://doi.org/10.1128/JCM.00932-16>.
- Brennan-Krohn T, Kirby JE. 2019. Antimicrobial synergy testing by the inkjet printer-assisted automated checkerboard array and the manual time-kill method. *JoVE* <https://doi.org/10.3791/58636>.
- Bhatnagar A, Boyd S, Sabour S, Bodnar J, Nazarian E, Peinovich N, Wagner C, Craft B, Snippes Vagnone P, Simpson J, Stone VN, Therrien M, Bateman A, Lower D, Huang JY, Gumbis S, Lonsway D, Lutgring JD, Karlsson M, Brown AC. 2021. Aztreonam-avibactam susceptibility testing program for metallo-beta-lactamase-producing Enterobacteriales in the antibiotic resistance laboratory network, March 2019 to December 2020. *Antimicrob Agents Chemother* 65:e0048621. <https://doi.org/10.1128/AAC.00486-21>.
- Ransom E, Bhatnagar A, Patel JB, Machado M-J, Boyd S, Reese N, Lutgring JD, Lonsway D, Anderson K, Brown AC, Elkins CA, Rasheed JK, Karlsson M. 2020. Validation of aztreonam-avibactam susceptibility testing using digitally dispensed custom panels. *J Clin Microbiol* 58:e01944-19. <https://doi.org/10.1128/JCM.01944-19>.
- Baron S, Hadjadj L, Rolain J-M, Olaitan AO. 2016. Molecular mechanisms of polymyxin resistance: knowns and unknowns. *Int J Antimicrob Agents* 48:583–591. <https://doi.org/10.1016/j.ijantimicag.2016.06.023>.
- Poirel L, Jayol A, Bontron S, Villegas M-V, Ozdamar M, Türkoglu S, Nordmann P. 2015. The mgrB gene as a key target for acquired resistance to colistin in *Klebsiella pneumoniae*. *J Antimicrob Chemother* 70:75–80. <https://doi.org/10.1093/jac/dku323>.
- Cheung CHP, Dulyayangkul P, Heesom KJ, Avison MB. 2020. Proteomic investigation of the signal transduction pathways controlling colistin resistance in *Klebsiella pneumoniae*. *Antimicrob Agents Chemother* 64:e00790-20. <https://doi.org/10.1128/AAC.00790-20>.
- Pillai S, Moellering R Jr, Eliopoulos G. 2005. Antimicrobial combinations, p 365–440. *In* Lorian V (ed), *Antibiotics in laboratory medicine*, 5th ed. Lippincott Williams & Wilkins, Philadelphia, PA.
- Leber A. 2016. Time-kill assay for determining synergy, p 5.14.3.1–5.14.3.6. *In* Leber A (ed), *Clinical microbiology procedures handbook*, 4th ed. ASM Press, Washington, DC.
- Hindler JA, Humphries RM. 2013. Colistin MIC variability by method for contemporary clinical isolates of multidrug-resistant Gram-negative bacilli. *J Clin Microbiol* 51:1678–1684. <https://doi.org/10.1128/JCM.03385-12>.
- McClelland M, Sanderson KE, Spieth J, Clifton SW, Latreille P, Courtney L, Porwollik S, Ali J, Dante M, Du F, Hou S, Layman D, Leonard S, Nguyen C, Scott K, Holmes A, Grewal N, Mulvaney E, Ryan E, Sun H, Florea L, Miller W, Stoneking T, Nhan M, Waterston R, Wilson RK. 2001. Complete genome sequence of *Salmonella enterica* serovar Typhimurium LT2. *Nature* 413:852–856. <https://doi.org/10.1038/35101614>.
- Ogawa W, Li D-W, Yu P, Begum A, Mizushima T, Kuroda T, Tsuchiya T. 2005. Multidrug resistance in *Klebsiella pneumoniae* MGH78578 and cloning of genes responsible for the resistance. *Biol Pharm Bull* 28:1505–1508. <https://doi.org/10.1248/bpb.28.1505>.
- Love MI, Huber W, Anders S. 2014. Moderated estimation of fold change and dispersion for RNA-seq data with DESeq2. *Genome Biol* 15:550. <https://doi.org/10.1186/s13059-014-0550-8>.
- Jeannot K, Bolard A, Plésiat P. 2017. Resistance to polymyxins in Gram-negative organisms. *Int J Antimicrob Agents* 49:526–535. <https://doi.org/10.1016/j.ijantimicag.2016.11.029>.
- Groisman EA. 2001. The pleiotropic two-component regulatory system PhoP-PhoQ. *J Bacteriol* 183:1835–1842. <https://doi.org/10.1128/JB.183.6.1835-1842.2001>.
- Cheng H-Y, Chen Y-F, Peng H-L. 2010. Molecular characterization of the PhoPQ-PmrD-PmrAB mediated pathway regulating polymyxin B resistance in *Klebsiella pneumoniae* CG43. *J Biomed Sci* 17:60. <https://doi.org/10.1186/1423-0127-17-60>.

37. Mitrophanov AY, Jewett MW, Hadley TJ, Groisman EA. 2008. Evolution and dynamics of regulatory architectures controlling polymyxin B resistance in enteric bacteria. *PLoS Genet* 4:e1000233. <https://doi.org/10.1371/journal.pgen.1000233>.
38. Danner RL, Joiner KA, Rubin M, Patterson WH, Johnson N, Ayers KM, Parrillo JE. 1989. Purification, toxicity, and antientotoxin activity of polymyxin B nonapeptide. *Antimicrob Agents Chemother* 33:1428–1434. <https://doi.org/10.1128/AAC.33.9.1428>.
39. Eckburg PB, Lister T, Walpole S, Keutzer T, Utley L, Tomayko J, Kopp E, Farinola N, Coleman S. 2019. Safety, tolerability, pharmacokinetics, and drug interaction potential of SPR741, an intravenous potentiator, after single and multiple ascending doses and when combined with β -lactam antibiotics in healthy subjects. *Antimicrob Agents Chemother* 63:e00892-19. <https://doi.org/10.1128/AAC.00892-19>.
40. Vaara M. 1992. Agents that increase the permeability of the outer membrane. *Microbiol Rev* 56:395–411. <https://doi.org/10.1128/mr.56.3.395-411.1992>.
41. MacNair CR, Stokes JM, Carfrae LA, Fiebig-Comyn AA, Coombes BK, Mulvey MR, Brown ED. 2018. Overcoming mcr-1 mediated colistin resistance with colistin in combination with other antibiotics. *Nat Commun* 9:458. <https://doi.org/10.1038/s41467-018-02875-z>.
42. Viljanen P, Vaara M. 1984. Susceptibility of Gram-negative bacteria to polymyxin B nonapeptide. *Antimicrob Agents Chemother* 25:701–705. <https://doi.org/10.1128/AAC.25.6.701>.
43. Delcour AH. 2009. Outer membrane permeability and antibiotic resistance. *Biochim Biophys Acta* 1794:808–816. <https://doi.org/10.1016/j.bbapap.2008.11.005>.
44. Chopra I, Hacker K. 1992. Uptake of minocycline by *Escherichia coli*. *J Antimicrob Chemother* 29:19–25. <https://doi.org/10.1093/jac/29.1.19>.
45. Nikaido H. 1998. The role of outer membrane and efflux pumps in the resistance of gram-negative bacteria. Can we improve drug access? *Drug Resist Updat Rev Comment Antimicrob Anticancer Chemother* 1:93–98. [https://doi.org/10.1016/S1368-7646\(98\)80023-X](https://doi.org/10.1016/S1368-7646(98)80023-X).
46. Zhang L, Dhillon P, Yan H, Farmer S, Hancock RE. 2000. Interactions of bacterial cationic peptide antibiotics with outer and cytoplasmic membranes of *Pseudomonas aeruginosa*. *Antimicrob Agents Chemother* 44:3317–3321. <https://doi.org/10.1128/AAC.44.12.3317-3321.2000>.
47. Sabnis A, Hagart KL, Klöckner A, Becce M, Evans LE, Furniss RCD, Mavridou DA, Murphy R, Stevens MM, Davies JC, Larrouy-Maumus GJ, Clarke TB, Edwards AM. 2021. Colistin kills bacteria by targeting lipopolysaccharide in the cytoplasmic membrane. *Elife* 10:65836. <https://doi.org/10.7554/eLife.65836>.
48. Humphrey M, Larrouy-Maumus GJ, Furniss RCD, Mavridou DA, Sabnis A, Edwards AM. 2021. Colistin resistance in *Escherichia coli* confers protection of the cytoplasmic but not outer membrane from the polymyxin antibiotic. *Microbiol Read Engl* 167:001104. <https://doi.org/10.1099/mic.0.001104>.
49. Dixon RA, Chopra I. 1986. Leakage of periplasmic proteins from *Escherichia coli* mediated by polymyxin B nonapeptide. *Antimicrob Agents Chemother* 29:781–788. <https://doi.org/10.1128/AAC.29.5.781>.
50. Aghapour Z, Gholizadeh P, Ganbarov K, Bialvaei AZ, Mahmood SS, Tanomand A, Yousefi M, Asgharzadeh M, Yousefi B, Kafili HS. 2019. Molecular mechanisms related to colistin resistance in Enterobacteriaceae. *Infect Drug Resist* 12:965–975. <https://doi.org/10.2147/IDR.S199844>.
51. Lippa AM, Goulian M. 2009. Feedback inhibition in the PhoQ/PhoP signaling system by a membrane peptide. *PLoS Genet* 5:e1000788. <https://doi.org/10.1371/journal.pgen.1000788>.
52. Schurek KN, Sampaio JLM, Kiffer CRV, Sinto S, Mendes CMF, Hancock REW. 2009. Involvement of pmrAB and phoPQ in polymyxin B adaptation and inducible resistance in non-cystic fibrosis clinical isolates of *Pseudomonas aeruginosa*. *Antimicrob Agents Chemother* 53:4345–4351. <https://doi.org/10.1128/AAC.01267-08>.
53. Spellberg B, Guidos R, Gilbert D, Bradley J, Boucher HW, Scheld WM, Bartlett JG, Edwards J, Infectious Diseases Society of America. 2008. The epidemic of antibiotic-resistant infections: a call to action for the medical community from the Infectious Diseases Society of America. *Clin Infect Dis* 46:155–164. <https://doi.org/10.1086/524891>.
54. Rojas LJ, Salim M, Cober E, Richter SS, Perez F, Salata RA, Kalayjian RC, Watkins RR, Marshall S, Rudin SD, Domitrovic TN, Hujer AM, Hujer KM, Doi Y, Kaye KS, Evans S, Fowler VG, Bonomo RA, van Duin D, Antibacterial Resistance Leadership Group. 2017. Colistin resistance in carbapenem-resistant *Klebsiella pneumoniae*: laboratory detection and impact on mortality. *Clin Infect Dis Off Publ Infect Dis Soc Am* 64:711–718. <https://doi.org/10.1093/cid/ciw805>.
55. Nation RL, Garonzik SM, Li J, Thamlikitkul V, Giamarellos-Bourboulis EJ, Paterson DL, Turnidge JD, Forrest A, Silveira FP. 2016. Updated US and European dose recommendations for intravenous colistin: how do they perform? *Clin Infect Dis* 62:552–558. <https://doi.org/10.1093/cid/civ964>.
56. Corbett D, Wise A, Langley T, Skinner K, Trimby E, Birchall S, Dorali A, Sandiford S, Williams J, Warn P, Vaara M, Lister T. 2017. Potentiation of antibiotic activity by a novel cationic peptide: potency and spectrum of activity of SPR741. *Antimicrob Agents Chemother* 61:e00200-17. <https://doi.org/10.1128/AAC.00200-17>.
57. Clinical and Laboratory Standards Institute. 2015. Methods for dilution antimicrobial susceptibility tests for bacteria that grow aerobically, 10th ed. Approved Standard M07-A10. CLSI, Wayne, PA.
58. Clinical and Laboratory Standards Institute. 2021. M100: performance standards for antimicrobial susceptibility testing, 31st ed. CLSI, Wayne, PA.
59. European Committee on Antimicrobial Susceptibility Testing. 2021. Breakpoint tables for interpretation of MICs and zone diameters. Version 11.0. https://www.eucast.org/fileadmin/src/media/PDFs/EUCAST_files/Breakpoint_tables/v_11.0_Breakpoint_Tables.pdf.
60. Alcock BP, Raphenya AR, Lau TTY, Tsang KK, Bouchard M, Edalatmand A, Huynh W, Nguyen A-LV, Cheng AA, Liu S, Min SY, Miroshnichenko A, Tran H-K, Werfalli RE, Nasir JA, Oloni M, Speicher DJ, Florescu A, Singh B, Faltyn M, Hernandez-Koutoucheva A, Sharma AN, Bordeleau E, Pawlowski AC, Zubyk HL, Dooley D, Griffiths E, Maguire F, Winsor GL, Beiko RG, Brinkman FSL, Hsiao WWL, Domselaar GV, McArthur AG. 2020. CARD 2020: antibiotic resistance surveillance with the comprehensive antibiotic resistance database. *Nucleic Acids Res* 48:D517–D525.
61. Bortolaia V, Kaas RS, Ruppe E, Roberts MC, Schwarz S, Cattori V, Philippon A, Allesoe RL, Rebelo AR, Florensa AF, Fagelhauer L, Chakraborty T, Neumann B, Werner G, Bender JK, Stingl K, Nguyen M, Coppens J, Xavier BB, Malhotra-Kumar S, Westh H, Pinholt M, Anjum MF, Duggett NA, Kempf I, Nykäsenoja S, Olkkola S, Wiecek K, Amaro A, Clemente L, Mossong J, Losch S, Ragimbeau C, Lund O, Aarestrup FM. 2020. ResFinder 4.0 for predictions of phenotypes from genotypes. *J Antimicrob Chemother* 75:3491–3500. <https://doi.org/10.1093/jac/dkaa345>.
62. Zankari E, Allesoe R, Joensen KG, Cavaco LM, Lund O, Aarestrup FM. 2017. PointFinder: a novel web tool for WGS-based detection of antimicrobial resistance associated with chromosomal point mutations in bacterial pathogens. *J Antimicrob Chemother* 72:2764–2768. <https://doi.org/10.1093/jac/dkx217>.
63. Camacho C, Coulouris G, Avagyan V, Ma N, Papadopoulos J, Bealer K, Madden TL. 2009. BLAST+: architecture and applications. *BMC Bioinformatics* 10:421. <https://doi.org/10.1186/1471-2105-10-421>.
64. Siguier P, Perchon J, Lestrade L, Mahillon J, Chandler M. 2006. ISfinder: the reference centre for bacterial insertion sequences. *Nucleic Acids Res* 34:D32–D36. <https://doi.org/10.1093/nar/gkj014>.
65. Chen CY, Nace GW, Irwin PL. 2003. A 6 x 6 drop plate method for simultaneous colony counting and MPN enumeration of *Campylobacter jejuni*, *Listeria monocytogenes*, and *Escherichia coli*. *J Microbiol Methods* 55:475–479. [https://doi.org/10.1016/S0167-7012\(03\)00194-5](https://doi.org/10.1016/S0167-7012(03)00194-5).
66. Bhattacharyya RP, Bandyopadhyay N, Ma P, Son SS, Liu J, He LL, Wu L, Khafizov R, Boykin R, Cerqueira GC, Pironti A, Rudy RF, Patel MM, Yang R, Skerry J, Nazarian E, Musser KA, Taylor J, Pierce VM, Earl AM, Cosimi LA, Shores N, Beechem J, Livny J, Hung DT. 2019. Simultaneous detection of genotype and phenotype enables rapid and accurate antibiotic susceptibility determination. *Nat Med* 25:1858–1864. <https://doi.org/10.1038/s41591-019-0650-9>.
67. Shishkin AA, Giannoukos G, Kucukural A, Ciulla D, Busby M, Surka C, Chen J, Bhattacharyya RP, Rudy RF, Patel MM, Novod N, Hung DT, Gnirke A, Garber M, Guttman M, Livny J. 2015. Simultaneous generation of many RNA-seq libraries in a single reaction. *Nat Methods* 12:323–325. <https://doi.org/10.1038/nmeth.3313>.
68. Li H, Durbin R. 2009. Fast and accurate short read alignment with Burrows-Wheeler transform. *Bioinformatics* 25:1754–1760. <https://doi.org/10.1093/bioinformatics/btp324>.
69. Robinson MD, McCarthy DJ, Smyth GK. 2010. edgeR: a Bioconductor package for differential expression analysis of digital gene expression data. *Bioinformatics* 26:139–140. <https://doi.org/10.1093/bioinformatics/btp616>.
70. McCarthy DJ, Chen Y, Smyth GK. 2012. Differential expression analysis of multifactor RNA-Seq experiments with respect to biological variation. *Nucleic Acids Res* 40:4288–4297. <https://doi.org/10.1093/nar/gks042>.

